

Hydraulic Fracturing and Seismicity in the Western Canada Sedimentary Basin

by Gail M. Atkinson, David W. Eaton, Hadi Ghofrani, Dan Walker, Burns Cheadle, Ryan Schultz, Robert Shcherbakov, Kristy Tiampo, Jeff Gu, Rebecca M. Harrington, Yajing Liu, Mirko van der Baan, and Honn Kao

ABSTRACT

The development of most unconventional oil and gas resources relies upon subsurface injection of very large volumes of fluids, which can induce earthquakes by activating slip on a nearby fault. During the last 5 years, accelerated oilfield fluid injection has led to a sharp increase in the rate of earthquakes in some parts of North America. In the central United States, most induced seismicity is linked to deep disposal of coproduced wastewater from oil and gas extraction. In contrast, in western Canada most recent cases of induced seismicity are highly correlated in time and space with hydraulic fracturing, during which fluids are injected under high pressure during well completion to induce localized fracturing of rock. Furthermore, it appears that the maximum-observed magnitude of events associated with hydraulic fracturing may exceed the predictions of an often-cited relationship between the volume of injected fluid and the maximum expected magnitude. These findings have far-reaching implications for assessment of induced-seismicity hazards.

INTRODUCTION

Recent studies have shown that a marked increase in the rate of earthquakes of moment magnitude (M) ≥ 3.0 in the central United States is largely attributable to the disposal of extraordinary volumes of coproduced wastewater from oil and gas operations, typically at 3–5 km depths (Ellsworth, 2013; Frohlich *et al.*, 2014; Keranen *et al.*, 2014; Hornbach *et al.*, 2015; Rubinstein and Babaie Mahani, 2015; Weingarten *et al.*, 2015). The moment release attributable to fluid-injection-induced earthquakes has been related to the net volume of injected fluid (McGarr, 2014). In contrast, Weingarten *et al.* (2015) argued that induced seismicity is more closely related to rates of injection. Some induced events are large enough to cause significant damage (Ellsworth, 2013; Keranen *et al.*, 2014), and thus induced seismicity is important to the assessment and mitigation of time-dependent hazards to people and infrastructure (Petersen *et al.*, 2015). In this regard, the maximum potential earthquake magnitude is of particular interest. McGarr (2014)

posited that maximum magnitude is controlled by the cumulative injected volume, whereas Sumy *et al.* (2014) argued that larger tectonic events may be triggered due to Coulomb stress transfer. Petersen *et al.* (2015) suggested using a large range of uncertainty to characterize maximum magnitude.

Based on these seminal studies of induced seismicity in the central United States, there is a growing tendency to consider wastewater injection operations as the primary concern in the assessment of induced-seismicity hazards (Petersen *et al.*, 2015; Rubinstein and Babaie Mahani, 2015). Hydraulic fracturing (HF), typically involving high-pressure injection of incremental volumes of fluids in multiple stages along horizontally drilled wells at 2–3 km depths, has been considered to play a relatively minor role in both the rate of induced events and their potential magnitudes (Holland, 2013; Skoumal *et al.*, 2015). Consequently, induced-seismicity hazards from hydraulic fracturing have often been inferred to be negligible compared with wastewater injection operations (National Research Council, 2013).

In general, the basic mechanism of induced seismicity by oil and gas operations involving fluid injection is well understood: an increase in pore-fluid pressure and/or a change in the state of stress may cause reactivation of existing faults or fractures (Healy *et al.*, 1968; Raleigh *et al.*, 1976). However, validated predictive models are not yet available to assess the likelihood, rates, or magnitudes of induced events from specific operations (National Research Council, 2013). New experimental results from fluid injection directly into a natural fault point to aseismic processes that can be modeled by a rate-dependent friction law as a precursor to seismic slip (Guglielmi *et al.*, 2015), hinting that in the future such models may be feasible. At present, however, models of induced-seismicity hazards are largely statistical in nature, typically relying on empirical analyses of the observed rate of induced events above a certain magnitude on a per-well basis (Atkinson, Ghofrani, and Assatourians, 2015; Weingarten *et al.*, 2015).

Canada is second only to the United States in terms of development of shale gas and shale oil resources (Energy Information Administration, 2013), with development focused primarily within the Western Canada Sedimentary Basin

(WCSB). In past decades, reported cases of induced seismicity in the WCSB have been attributed to stress changes from hydrocarbon production (Baranova *et al.*, 1999), enhanced oil recovery (Horner *et al.*, 1994), and wastewater disposal (Schultz *et al.*, 2014). The pace of unconventional resource development has accelerated in the WCSB in the last five years due to the deployment of new technologies, particularly the widespread drilling of horizontal wellbores, up to several kilometers in length, in which production is stimulated by multistage hydraulic fracturing. Recent evidence suggests that hydraulic fracturing plays a significant role in triggering seismicity in western Canada (B.C. Oil and Gas Commission, 2012, 2014; Eaton and Babaie Mahani, 2015; Atkinson, Assatourians, *et al.*, 2015; Farahbod *et al.*, 2015; Schultz, Mei, *et al.*, 2015; Schultz, Stern, Novakovic, *et al.*, 2015) in marked contrast to the putative mechanism in the central United States

In this article, we systematically examine whether a robust correlation exists between seismicity and hydraulic fracturing in the WCSB. We do not aim to prove a causal connection between any particular hydraulic fracture (HF) well and any particular earthquake; rather, we provide a broad-level overview of the spatiotemporal relationship between HF operations and seismicity to make preliminary estimates of how commonly earthquakes should be expected to occur in proximity to such operations. As we elaborate below, we find a high level of correlation in both time and space, which is very unlikely to be coincidental. Moreover, we show that in most cases the correlation is unlikely to be related to any nearby disposal wells. We determined this by looking also at the relationship between seismicity and disposal wells in the WCSB. We discuss our findings of the correlation between HF wells and seismicity in light of a conceptual model for diffusion of pore pressures caused by hydraulic fracturing and also discuss the relationship between the magnitude of events and volumes of fluid used in the treatment programs. The causative details of the correlation between hydraulic fracturing and seismicity, in terms of how it works on the level of specific wells, formations, and tectonic regimes are beyond our current scope, but can be explored in future case studies.

THE RELATIONSHIP BETWEEN SEISMICITY AND OIL AND GAS WELLS

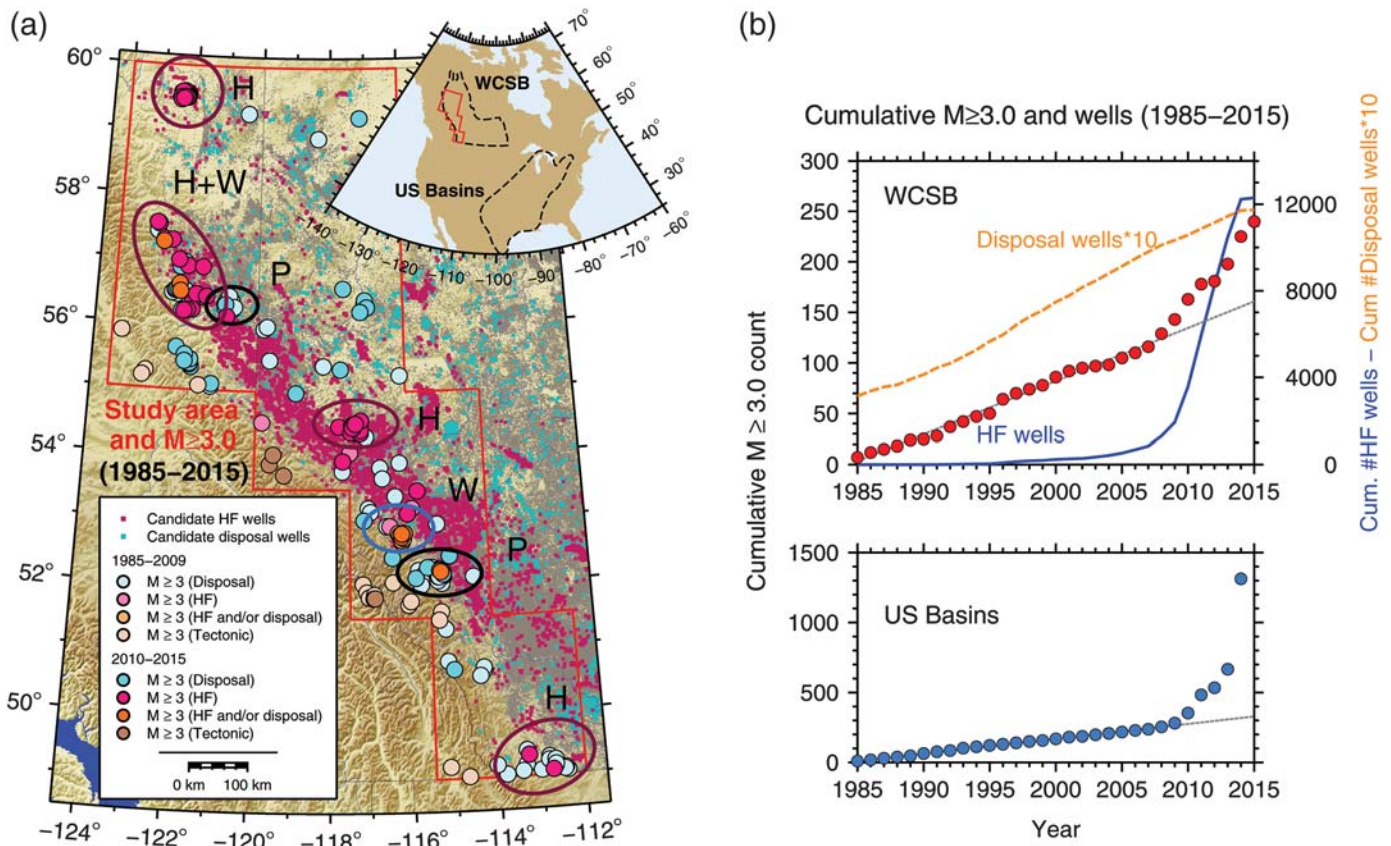
We examine the statistical relationship between oil and gas activity and seismicity in the WCSB from 1985 to 2015, using a compiled database of seismicity and a compiled database of hydraulically fractured wells and disposal wells, covering the time period from 1985 to June 2015 (see [Data and Resources](#)). Our geographic focus parallels the foothills region of the WCSB, within an area of approximately 454,000 km² near the border between Alberta and British Columbia; this is the study area as shown in [Figure 1](#). Seismicity data were obtained from the Composite Seismicity Catalogue for the WCSB; all magnitudes are moment magnitude (M). The catalog is believed to be complete in the study area from 1985 at the $M \geq 3$ level, as documented by the Geological Survey of Canada (Adams and

Halchuk, 2003), but completeness at lower magnitude levels varies in time and space (e.g., Schultz, Stern, Gu, *et al.*, 2015). The database of ~500,000 wells (all types) from 1985 to 4 June 2015, as obtained from the Alberta Energy Regulator and the B.C. Oil and Gas Commission, was searched using geoSCOUT software (geologic systems Ltd.). This database was also accessed to obtain injected fluid volumes for disposal wells and for HF treatment stages. Net injected volume for HF wells is calculated assuming 50% recovery of hydraulic fracturing fluids (B.C. Oil and Gas Commission, 2014).

[Figure 1](#) shows the locations of wells and earthquakes used in this study (see [Data and Resources](#)). The examined wells include multistage horizontal HF wells and water disposal wells that have potentially significant net fluid volume; these disposal wells are chiefly for disposal of wastewater (not enhanced oil recovery). We focused on horizontal wellbores in considering the relationship between seismicity and hydraulic fracturing, because horizontal drilling favors fault activation to a greater degree than do vertical wellbores. A set of proximal horizontal wells in multistage completion will impact a significantly greater volume than will a single vertical well, thus increasing the probability of perturbing the pore pressure or stress environment of a fault. In total, 12,289 HF wells and 1236 disposal wells lie within the study area. (The seismicity database for 2015 represents less than half of a year to 4 June 2015 and the database for the wells is incomplete in the latter part of 2014 and for 2015, owing to the allowable time lag between completion of HF operations and reporting of the information to the regulator.) It can be seen in [Figure 1](#) that seismicity in the WCSB has increased markedly starting in about 2009, synchronous with a large increase in the number of HF treatments completed in horizontal wells. By comparison, the number of wastewater disposal wells has increased at a more constant rate. The sharp increase in HF wells has not required a correspondingly sharp increase in the number of disposal wells, in part because the WCSB does not include large de-watering plays that involve transfer of massive volumes of coproduced wastewater into hydrologically isolated formations (Rubinstein and Babaie Mahani, 2015). Such massive transfers of formation fluids are a key characteristic of oil production in parts of the central United States, particularly Oklahoma (Murray, 2013; Walsh and Zoback, 2015; Weingarten *et al.*, 2015).

Hydraulic Fracture Wells

[Figure 1](#) motivates us to further examine the apparent correlation between the increase in HF wells and the increase in the rate of $M \geq 3$ earthquakes in the WCSB. To test if there is spatial and temporal correlation between HF wells and seismic events, we performed an initial screening to flag all $M \geq 3$ earthquakes having a reported location within a 20 km radius of each HF well. The choice of initial flagging criteria is deliberately broad, based on the following considerations: (1) the typical location uncertainty of catalog events, until very recently, is ~15 km in many areas of the WCSB, as evidenced by discrepancies in event locations quoted by different agencies for the same events (see [Data and Resources](#) for catalog docu-



▲ Figure 1. Seismicity and wells in the Western Canada Sedimentary basin (WCSB). (a) Red lines delineate the study area, which parallels the foothills region of the WCSB. Ovals identify areas where induced seismicity has been previously attributed to hydraulic fracturing (H), wastewater disposal (W), and production (P). Red/pink circles show $M \geq 3$ earthquakes correlated with hydraulic fracture (HF) wells. Turquoise circles show $M \geq 3$ earthquakes correlated with disposal wells. Orange circles are correlated with both. Small squares in the background show locations of examined HF wells (dark pink) and disposal wells (turquoise). Gray squares in the far background are all wells. (b) Cumulative rate of seismicity within the WCSB, commencing in 1985; numbers of disposal wells and HF wells for the WCSB as compiled in this study are indicated (top). A roughly synchronous increase in rate is evident in the basins of the central and eastern United States (bottom; data plotted from Ellsworth, 2013) (Well information is not available in the Ellsworth study, but most activity is considered to be related to wastewater disposal.) The gray lines show the expected counts for a constant seismicity rate.

mentation); (2) HF wells may be several kilometers in lateral extent; and (3) events may be induced at distances up to a few kilometers from the causative well, as the fluid pressures diffuse along local faults and fractures (discussed further below; Fig. A1). We emphasize that the initial 20-km distance limit is strictly for the purpose of flagging for study those events that might have occurred within a short distance (~ 1 km) of an HF well, considering location uncertainty. Once a potential spatial correlation is identified, a check is made for a temporal relationship. We consider that a temporal correlation may exist if an event occurred within a window beginning with the commencement of hydraulic fracturing and ending 3 months after the completion of treatment (the HF window). This time window was selected based on maximum time lags reported for a representative subset of our study area in the the Horn River basin (Farahbod *et al.*, 2015). Again, we emphasize that we begin with a relatively broad time window to flag events and wells for further study.

In some cases, due to lack of specific information in the public databases, it was necessary to estimate the start and stop dates of the HF window based on indicative well information, such as the date that drilling was completed and the date that the well began production; typically, HF treatments commence a few days after the drilling has been completed, whereas production typically commences within a few days to weeks following the treatment program. Refractured wells, in which hydraulic fracturing stimulation is repeated to renew production levels in a previously treated well, are not considered in our analysis, but could be important in areas where refracturing is used more extensively than is the case for the WCSB.

The initial screening flagged 52 HF wells (out of a total of 12,289) as being potentially correlated with $M \geq 3$ seismicity. (This number was later reduced to 39, following the secondary screening.) These wells include a number of cases of seismicity believed to be induced by hydraulic fracturing that have already been discussed in the literature, such as the 2011–2012 Card-

ston swarm (Schultz, Mei, *et al.*, 2015), the December 2013 Fox Creek event (Schultz, Stern, Novakovic, *et al.*, 2015), the 16 July 2014 and 30 July 2014 Montney events (B.C. Oil and Gas Commission, 2014), the events in the Horn River basin (B.C. Oil and Gas Commission, 2012), the January 2015 Fox Creek event (Schultz, Stern, Novakovic, *et al.*, 2015), and the 4 August 2014 Montney event (B.C. Oil and Gas Commission, 2014). We are unaware of any sequences identified in the literature that were not also flagged by our screening criteria.

Because the initial screening criteria are relatively broad in time and space, one could argue that the correlation that we obtain between HF wells and seismicity might be similar to that expected by random chance. To investigate whether this is so, we performed a Monte Carlo analysis. We consider the study area (Fig. 1) as an areal source zone in the context of a classic probabilistic seismic-hazard analysis (PSHA; Cornell, 1968; Adams and Halchuk, 2003). The zone has the observed rate of 240 earthquakes of $M \geq 3$ in the study period (1985–June 2015). We first invoke the classical PSHA assumption (as used in the national seismic-hazard mapping program in Canada) that the catalog of events in this time period is distributed randomly in time and space, with the observed catalog representing one random realization. We use a Monte Carlo earthquake simulation approach (EQHAZ1, Assatourians and Atkinson, 2013) to simulate 5000 independent earthquake catalogs for the study area and time period. Each of these simulated catalogs has 240 events of $M \geq 3$, distributed randomly in time and space according to a classic hazard analysis for an areal source zone, in which seismicity is assumed to be a Poisson process (e.g., Adams and Halchuk, 2003). We determine how many of our candidate HF wells pass the initial screening criteria (in time and space) for each catalog. We order the 5000 results to determine the likelihood of obtaining our observed frequency of correlation with the initial screening criteria by random chance.

The frequency of having 52 HF wells (or more) pass the initial screening criteria by chance is $\ll 1\%$, because the maximum number of associated HF wells that we obtain in 5000 trials is 43. The 10th to 90th percentile range for the number of HF wells that pass the initial screening criteria is 19–31; the median is 25. This suggests that of our 52 flagged HF wells, only about half of this number are expected to be flagged by our initial screening criteria just by random chance, if we assume that earthquakes follow a process by which they are randomly distributed in time and space.

The above analysis is somewhat simplistic, as it is known that earthquakes tend to cluster in space, as some areas are more prone to seismicity than others. It is possible that oil and gas resources happen to be concentrated in the same areas where tectonic earthquakes are concentrated. To test whether this might explain the apparent correlation of HF wells and seismicity, we repeat the Monte Carlo analysis but use a more realistic seismicity model that reproduces the observed earthquake clustering in the catalog. We use the observed seismicity from 1985 to the end of 2009 to define the spatial clustering (and rate) of events of $M \geq 3$. The idea is to test whether the observed correlation of seismicity with HF wells in the 2010–

2015 period is consistent with the historical patterns of seismicity and seismic hazard as observed prior to the widespread implementation of HF wells. For this purpose, we use the smoothed-seismicity option in the seismic-hazard algorithm EQHAZ1 (Assatourians and Atkinson, 2013), which follows the Frankel (1995) methodology in clustering the likelihood of the events in space, according to their observed clustering in the catalog. In accordance with standard practice in evaluating hazard from natural seismicity, a correlation distance of 50 km is used in the algorithm for simulating seismicity of $M \geq 3$, with a ring width of 10 km for the smoothing kernel (see Frankel, 1995, for details). We determined how many of our HF wells pass the screening criteria (in time and space) for each catalog generated with the observed spatial clustering of the actual catalog (as determined from observed seismicity to 2010). In 5000 random trials under the smoothed-seismicity model, the 10th to 90th percentile number of hits was 7–14. The reason that this number is less than for the uniform seismicity model is two-fold: (1) the rate of seismicity increased, beginning in 2010, relative to the pre-2010 model and (2) the locations of events from 2010 to 2015 do not follow the pattern established before that time. Thus, if we postulate that the spatial clustering of events near HF wells could be due to tectonic or other causes, the temporal relationship is even more unlikely to be a matter of random chance.

It may be argued that some other factor is responsible for the spatiotemporal relationship between HF wells and seismicity. The most likely candidate would be disposal wells, given the widespread evidence in the United States for such an association. Specifically, we considered the possibility that the rate of injection in disposal wells underwent an increase that was synchronous with HF operations nearby, and this is the reason why seismicity increases in close proximity in time and space to HF well operations. To test the hypothesis that disposal is triggering the seismicity near HF wells, we identified all disposal wells within 20 km of each of the $M \geq 3$ events that were flagged as being potentially correlated with HF wells. If there is no disposal well with significant activity that predates the seismicity, this is not a possible explanation for that event. We consider the disposal activity to be significant if the minimum disposal volume, prior to seismicity initiation, is at least 10,000 m³. The selected minimum volume is of the order of that involved in typical HF operations (e.g., Schultz, Mei, *et al.*, 2015), and on the low end of the range considered by McGarr (2014) for an injection-induced $M \geq 3$ event. To ensure consistent temporal criteria, we checked whether the minimum volume (or more) was injected in the disposal well in the same 3-month window preceding the event that was used for the HF wells. For most disposal wells, the operations are ongoing, and so volumes of this order may have been injected continuously over a period of years, with cumulative volumes being orders of magnitude higher. Thus, the three-month window is a test to determine whether nearby disposal wells contributed at least as much fluid to the crust as did the HF treatments in the same time window. If so, the disposal well may be the more important factor, and we need to look in

more detail at the spatial and temporal relationship of the seismicity to both HF wells and disposal wells.

To evaluate the wells more carefully, we manually examine the spatiotemporal correlation of seismicity within the 20 km radius and HF treatment windows for all 52 initially flagged HF wells. The aim is to determine whether a correlation of the observed seismicity with the HF wells is reasonable, or whether the association is just as likely to be due to a nearby disposal well. To enrich the database of available events with which to evaluate the correlation, we consider for this purpose the occurrence of all events in the catalog having $M \geq 2$. The use of this additional information greatly enhances our ability to discriminate clusters of seismicity from isolated events, enabling more confident association of specific wells with seismicity. The catalog is not complete to $M 2$ in most areas until very recently, but this is not critical for the specific purpose of examining the initiation and growth of event clusters in the narrow time window surrounding a HF well treatment; we simply acknowledge that the catalog of examined events may be incomplete for $M < 3$.

When events occur in proximity to both disposal wells and HF wells, we consider a correlation with HF wells likely if: (1) seismicity in the area around the disposal well (within ~ 40 km) was uncommon before hydraulic fracturing began and (2) the events cluster within the limited time periods represented by the HF windows and within the 20 km HF radius. We also searched the technical literature to investigate whether there was additional information that was more definitive. We would have liked to consider focal depth as a discriminant, but for most events in the catalog, the depth is not sufficiently well determined to pursue such a strategy. By carefully examining each identified HF well that is potentially correlated with seismicity, using the additional information as outlined above, we greatly increase our confidence in the association rate. Nevertheless, we acknowledge that the potential remains for some false positives. On the other hand, there is also significant potential to miss associated events, because the publicly available databases of HF wells are incomplete. In rare cases where an event is potentially associated with more than one HF well, we arbitrarily assign it to the closest well to avoid double counting of induced events.

Figure 2 presents a typical example of earthquakes that were within 20 km of both an HF well and a disposal well, but which we have flagged as being associated with HF wells following secondary screening. All of the events occurred within an HF time-and-distance window. No events occurred before the HF wells began in the area (in 2011), nor after the HF windows finished. Moreover, the disposal volumes are low and are relatively stable (until a recent increase in disposal rate, which did not begin until after the events). This suggests to us that the events in this area are much more likely to be related to HF wells than to the disposal well. Of the 52 flagged HF wells, we concluded that for 39 HF wells the activity does not appear to be related to any disposal well. We identified one HF well where the initially associated seismicity is much more likely to be associated with a nearby disposal well. We identified 12 HF

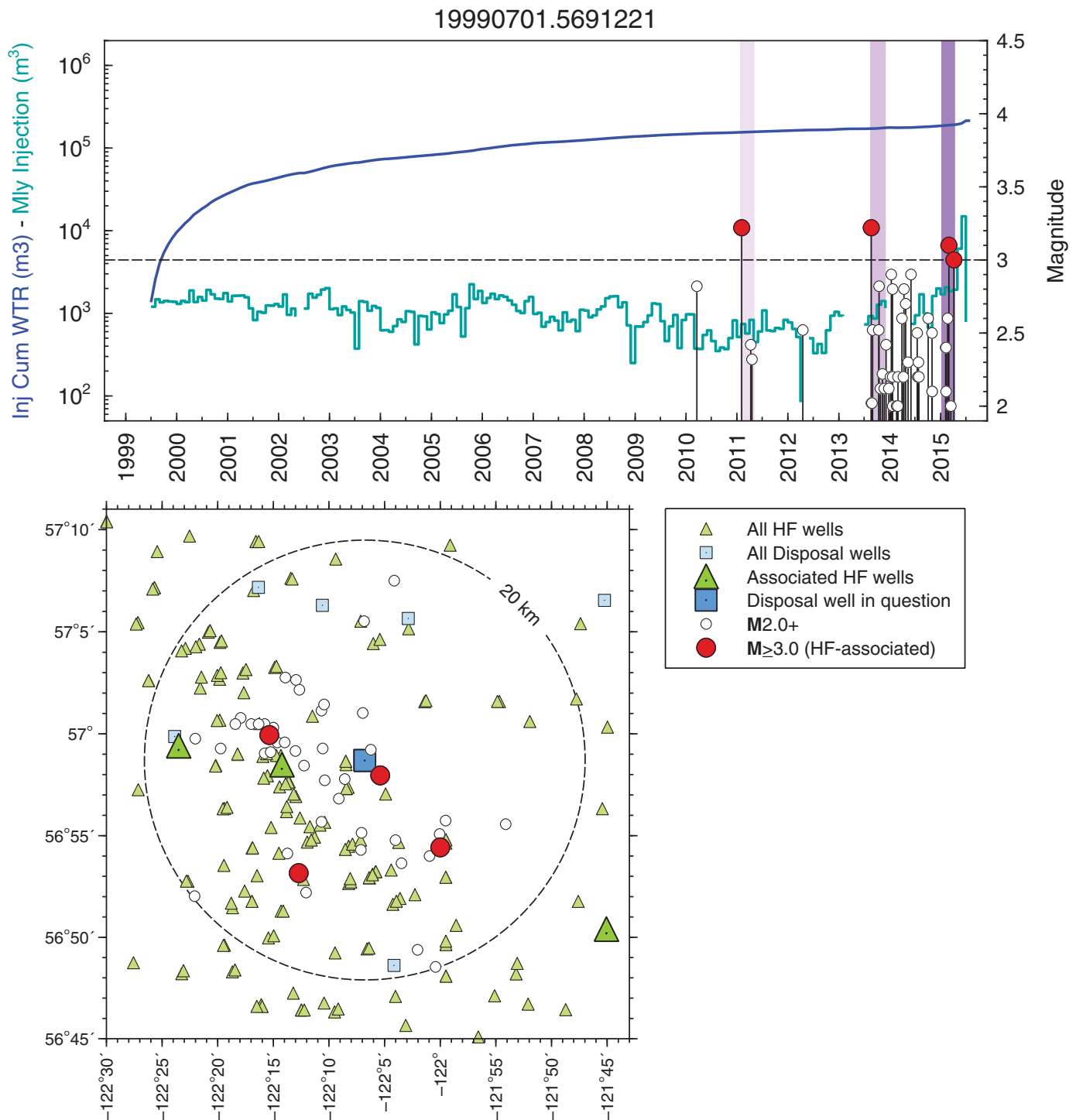
wells for which the associated seismicity is just as likely to be related to a nearby disposal well, and so an association of the events with HF wells is ambiguous. We did not count these HF wells as associated, but there is an interesting possibility that some events may be triggered by the combined effects of fluids injected from HF operations and nearby disposal operations.

Figure 3 presents an example for which the seismicity that passed the initial screening criteria for HF wells is much more likely to be related to a nearby disposal well. A nearby disposal well has been operating since 1971, and there have been frequent clusters of events in the vicinity. It is likely coincidental that several events occurred in the two HF windows that are within 20 km of the disposal well.

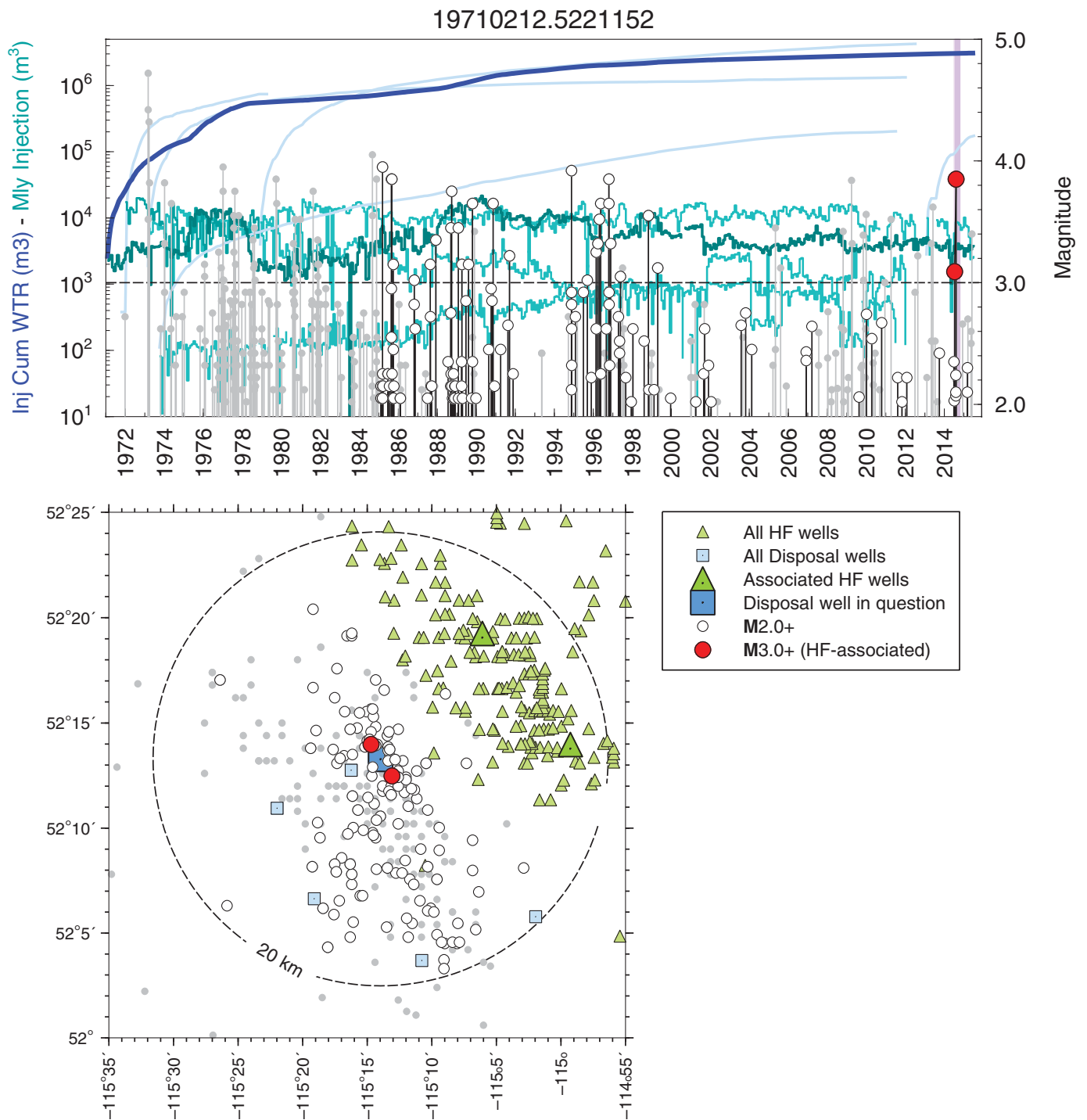
All associations made in Figure 1 and Table 1 between wells and seismicity are based on the more detailed well-by-well screening, aided by analysis such as illustrated in examples provided in Figures 2 and 3. For the 39 HF wells for which the seismicity does not appear to be related to disposal (or coincidental), the average distance from the well to the nearest associated event is 11 km (with a standard deviation of 5 km); this is a reasonable distribution when interpreted as representing the average uncertainty in epicentral location. For those events that we have classed as being correlated with HF wells, there is a bimodal temporal distribution. A peak of associated events occurs within 10 days of the HF treatment, then a second broader peak in the distribution that spans the time period from 30 to 90 days, with a small tail extending to longer time periods. This is in accord with the postulated bimodality of the event-triggering mechanisms, wherein events may be triggered during the treatment phase if a fault is encountered or may be triggered later as pore pressure diffuses over the area.

Although the well-by-well screening improves our confidence in the correlations made in Table 1, we acknowledge that an element of subjectivity remains, and cases may exist in which an apparent correlation is entirely coincidental, or where a disposal well is also involved. Finally, we likely missed events that were associated with HF wells because the well information in the public databases is incomplete. Thus, we consider our association rates to be uncertain, perhaps by as much as a factor of two.

In summary, out of 12,289 candidate HF wells, we identify 39 as being correlated with $M \geq 3$ seismicity, or approximately 0.3% as an average across the region. Based on the Monte Carlo analysis (considering smoothed seismicity), 7–14 wells were identified just by random chance, and our secondary screening may not have filtered all of these; thus we may have a few false positives that have inflated the count. On the other hand, we did not include an additional 12 HF wells that in the count because they are near a disposal well that could be involved. Moreover, some HF wells are known to be missing in the database, and of course these would not be counted. Considering these uncertainties, the actual percentage of HF wells that correlate in time and space with $M \geq 3$ seismicity is likely in the 0.2%–0.4% range regionally (e.g., 30–50 of 12,289 wells). A more detailed analysis of the attributes of the associated wells should be made in future studies. For example, we note that associated wells are in all of the most common formations



▲ **Figure 2.** Example of events that met initial screening criteria for HF wells but are also within 20 km of a disposal well. These events are classed in secondary screening as being correlated with the HF wells, due to the temporal relationship of events with HF windows and lack of previous seismicity within 20 km of the disposal well. The red dots show the timing of $M \geq 3$ HF-flagged earthquakes within the 20 km radius of the disposal well and their magnitude (at right). The HF window is 3 months (purple bars). The title gives date that the nearby disposal well group began operations (the digits before the decimal place) and a key to latitude and longitude of well (the digits following the decimal, in this case referring to 56.9° N, 122.1° W). The blue line shows the cumulative injected water (m^3), and the turquoise line shows the monthly (Mly) injection (m^3).



▲ **Figure 3.** Example of events that met initial criteria for HF wells that were subsequently classed as being related to disposal during secondary screening (red dots); temporal relationship of $M \geq 3$ events within HF windows (red dots) appears coincidental, considering other events (white dots) within a 20 km radius of the nearest disposal well group (blue square); solid gray dots show other nearby events that do not fall within the time–distance window for the highlighted disposal well but might be related to other nearby disposal wells (smaller blue squares). Title gives the key to well date and event location (as in Fig. 2).

under development (e.g., Duvernay, Montney, Cardium formations), but further study of the details of correlations in different formations, at different depths, and under different tectonic conditions is warranted.

Maximum Observed Sizes of Events from Hydraulic Fracturing in the WCSB

By considering slip on a (nearly) critically stressed fault in response to an increase in pore pressure, [McGarr \(2014\)](#) argued

Table 1
Summary of Seismicity Associated with Wells
in the Western Canada Sedimentary Basin

	Disposal	HF	Tectonic $M \geq 3$
Number of candidate wells (1985–2015)	1236	12,289	—
Number of wells associated with $M \geq 3$	17	39	—
Association % for wells ($M \geq 3$)	~1%	~0.3%	—
Number of $M \geq 3$ (1985–2009)	126*	13*	14
Number of $M \geq 3$ (2010–2015)	33*	65*	7
Association % for $M \geq 3$ (2010–2015)	31%	62%	7%

*These totals each include 18 events for which both disposal and hydraulic fracture (HF) wells could be associated, 8 of which occurred from 2010 to 2015; in assessing % association rates, each such event has been counted as ½. See [Data and Resources](#) for lists of associated wells and events.

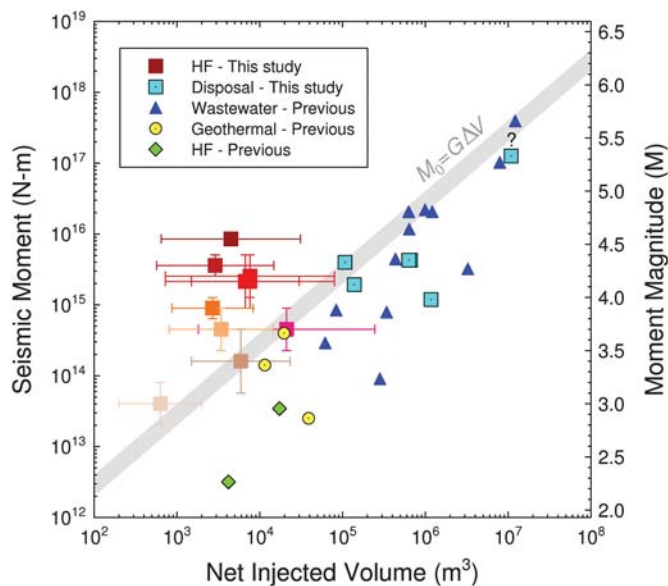
that the maximum seismic moment for an injection-induced earthquake can be approximated by the product of net injected volume and the shear modulus. This relationship appears to bound observations from wastewater disposal and geothermal operations. Seismic moment scales as the product of rupture area and average slip; consequently, an implicit assumption of the McGarr model is that injected fluid volume constrains the portion of the total fault surface that may slip during an induced event. However, the existence of a correlation between volume and maximum observed magnitude is also consistent with the concept that pore-pressure diffusion over a larger volume of the subsurface increases the likelihood of intersection with critically stressed faults (Shapiro and Dinske, 2009). Thus, the observed correlation could be primarily statistical in nature, rather than physical.

Seven particularly well-known cases in the WCSB have been documented on a case-by-case basis, for which induced seismicity is highly likely to have been caused by hydraulic fracturing operations. These are the 2011–2012 Cardston swarm (Schultz, Mei, *et al.*, 2015), December 2013 Fox Creek event (Schultz, Stern, Novakovic, *et al.*, 2015), 16 July 2014 and 30 July 2014 Montney events (B.C. Oil and Gas Commission, 2014), Horn River basin events (B.C. Oil and Gas Commission, 2012), January 2015 Fox Creek event (Schultz, Stern, Novakovic, *et al.*, 2015), and 4 August 2014 Montney event (B.C. Oil and Gas Commission, 2014). Moreover, since the initial submission of this study, three additional events of $M \sim 4$ –4.5 have occurred: the June 2015 Fox Creek event, the August 2015 Fort St. John event, and the January 2016 Fox Creek event. We compare the information from these

10 events with the proposed relation of McGarr (2014) between maximum magnitude and volume in Figure 4. To prepare this figure, we used alternative estimates of moment available in the literature sources cited, supplemented by regional moment tensor solutions provided by Nanometrics, Inc. (Andrew Law, personal comm., 2015) and the Pacific Geoscience Centre (Honn Kao, personal comm., 2015). For the most recent events, we also included regional moment tensor solutions obtained by University of Alberta (Jeff Gu, personal comm., 2015), and by University of Calgary (Dave Eaton, personal comm., 2015). These alternative moment magnitudes tend to span a range of up to 0.4 units, due to the use of different stations and different velocity models.

The volume estimates raise the interesting question of what volume should be summed. The volume for the stage that took place just before the event occurred is our minimum estimate of the volume; this single-stage volume would place most of these events above the plotted upper bound of McGarr (2014). It may be more reasonable to sum the volume over all stages of the HF operation (up to the time of the event); this sum is our maximum volume. For some events (those near Fort St. John), several HF wells were operating in close proximity in time and space (within a few kilometers and a few days); in these cases we summed the volumes from all proximate wells to obtain the maximum volume. In all cases, the injected volume has been multiplied by an estimated recovery factor of 0.5 to represent the actual fluid volume that may have migrated away from the treatment zone. (For the January 2016 event, the details of fluid volumes are not yet available; this point has been plotted by assuming the volume range is similar to other contemporary treatments in the same area and the same formation.)

An inspection of Figure 4 reveals that for several events the observed magnitude exceeds the maximum bounds provided by the McGarr relation. For many of the events above the McGarr line, we acknowledge that use of the maximum value of volume might just allow the point to come beneath the line. However, a few two events are clearly above the line, even with the combination of the maximum volume and the minimum magnitude; these are August 2014 M 4.4 and August 2015 M 4.6 events near Fort St. John (B.C. Oil and Gas Commission, 2014, 2015). Because these points are important, we provide more information on the data used to plot them. The volume estimates come from the B.C. Oil and Gas Commission (Dan Walker, personal comm., 2015) and are the volumes reported directly to them, according to provincial regulations, by the well operators; maximum volumes include the sum over all proximate operations in time and space. The M estimates for the 2014 event range from the regional moment tensor value (upper value) of 4.4 reported by the Pacific Geoscience Centre and U.S. Geological Survey (USGS) to lower values of M 4.2 obtained from ground-motion amplitude data and alternative regional moment tensor values (see Atkinson, Asatourians, *et al.*, 2015). For the 2015 event, the M estimates range from the Pacific Geoscience Centre and USGS regional moment tensor value of 4.6 to the value of 4.5 obtained using



▲ **Figure 4.** Net injected fluid volume versus seismic moment (in N·m on left axis, equivalent M on the right axis). Observations of induced seismicity from various mechanisms are compared to the maximum magnitude predicted by the McGarr (2014) upper-bound relation (shown as a shaded gray band that spans the range from 20–40 GPa for the assumed value of shear modulus G). The data-points from previous studies for wastewater (blue triangles), geothermal (yellow circles), and HF (green diamonds) are extracted from McGarr (2014). Hydraulic fracturing examples in this study are indicated by solid squares (red to tan), with error bars that show the uncertainty in the range of net injected volume from the stage prior to event occurrence (minimum) to the sum of volumes for all stages for all proximal well completions for a period of one month preceding the event (maximum), as well as the assessed uncertainty in seismic moment of each event, considering alternative estimates of magnitude from alternative agencies; the squares show the center of the uncertainty range in M and volume for HF-induced events. Examples are, from bottom to top: Cardston swarm (Schultz, Mei, et al., 2015), December 2013 Fox Creek event (Schultz, Stern, Novakovic, et al., 2015); 16 July 2014 and 30 July 2014 Montney events (B.C. Oil and Gas Commission, 2014); Horn River Basin (B.C. Oil and Gas Commission, 2012); January 2015 Fox Creek (Schultz, Mei, et al., 2015), and June 2015 Fox Creek events (R. Schultz, personal comm., 2016); 12 January 2016 Fox Creek event (H. Kao, J. Gu, D. Eaton, and A. Law, personal comm., 2016); 4 August 2014 Montney event (B.C. Oil and Gas Commission, 2014); 17 August 2015 Montney event (B.C. Oil and Gas Commission, 2015).

1 Hz ground motions, as described by Novakovic and Atkinson (2015).

We conclude from Figure 4 that the McGarr (2014) postulated relationship between maximum magnitude and injected fluid volume may not be applicable to earthquakes induced by hydraulic fracturing in the WCSB. Rather, we propose that the size of the available fault surface that is in a critical state of stress may control the maximum magnitude. As oil and

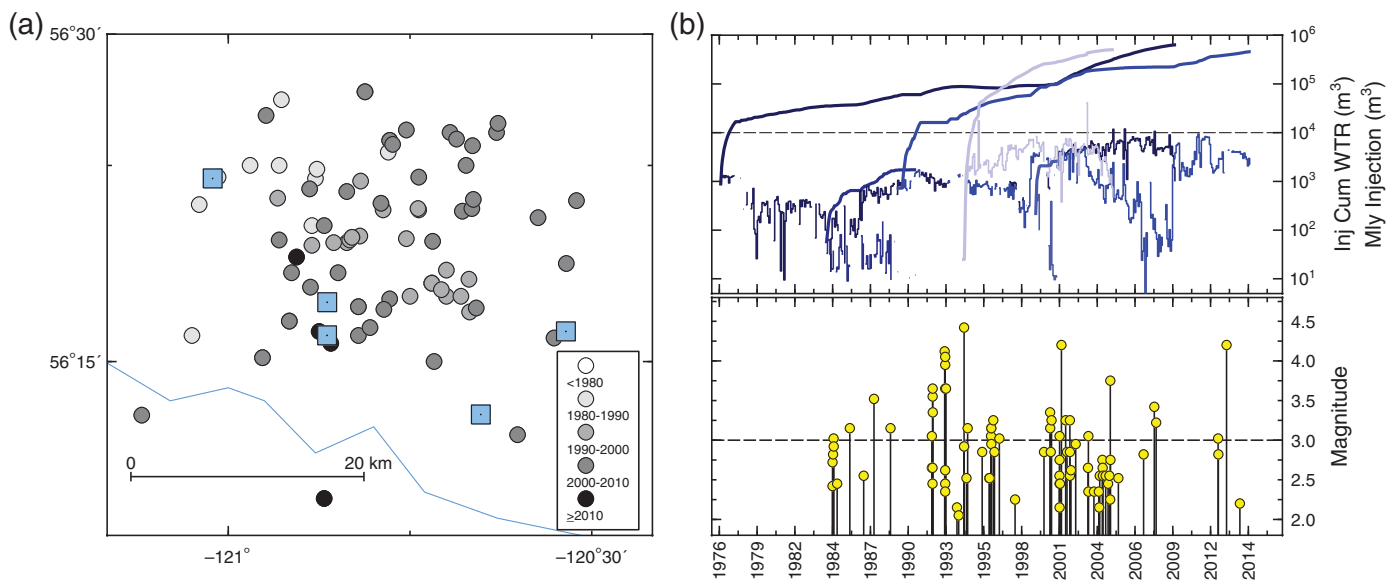
gas activities continue, and an increasingly large crustal volume is affected by increased pore pressures, we expect that more earthquakes will occur, at least in some areas (Farahbod et al., 2015), and their maximum magnitudes may exceed the values observed to date. It is therefore important to gain a better understanding of the potential magnitude distribution of events that may be induced by hydraulic fracturing.

Implications of Diffusion Characteristics of Hydraulic Fracturing

Fault activation due to hydraulic fracturing can occur directly or indirectly. If an expanding HF intersects a pre-existing fault, slip can be triggered immediately due to injection of fluids directly into the fault (Maxwell et al., 2008; Guglielmi et al., 2015). This corresponds to the minimum volume scenarios used in Figure 4. In this scenario, it is expected that termination of applicable treatment stage(s) (B.C. Oil and Gas Commission, 2012) should constitute an effective mitigation strategy. It is also possible for fault activation to occur indirectly, by diffusion of pore pressure away from the injection zone in a manner that is similar, in principle, to induced seismicity caused by fluid diffusion from a disposal well (Raleigh et al., 1976; B.C. Oil and Gas Commission, 2012; Keranen et al., 2014); this corresponds to the maximum volume scenario used in most cases in Figure 4. In this case, the magnitude and timing of the seismicity induced by hydraulic fracturing could be related to the total volume of injected fluids, as has been observed in the Horn River area of British Columbia (Farahbod et al., 2015). Because of differing spatial and temporal design characteristics, however, fundamental differences exist between the pore-pressure diffusion signatures of wastewater injection and hydraulic fracturing. Current industry practice for wastewater disposal in the WCSB involves injection significantly below breakdown pressure, typically in a single vertical well that is perforated within a permeable formation (B.C. Oil and Gas Commission, 2014). In contrast, hydraulic fracturing fluids are injected above formation breakdown pressure, typically into rock units with exceptionally low matrix permeability, in multiple stages and over a large area ($> 1 \text{ km}^2$). To elucidate these different pore-pressure diffusion signatures, we numerically simulated diffusion of pore pressure within a poroelastic medium. As shown in the Appendix, the pore-pressure signature from a multistage HF well operation may extend about a kilometer or so from the well and may persist for more than a month. This indicates the potential for several nearby wells to all contribute to the triggering of an event on a proximate fault; this is the maximum volume scenario considered in Figure 4 for events in the Montney.

Disposal Wells

We next examine the correlation between seismicity and disposal wells. This is an inherently different exercise, as no well-defined time window for correlation exists. It has been shown that disposal wells can induce seismicity at large distances and over time periods of decades (Keranen et al., 2013, 2014). To identify disposal wells that may be associated with seismicity,

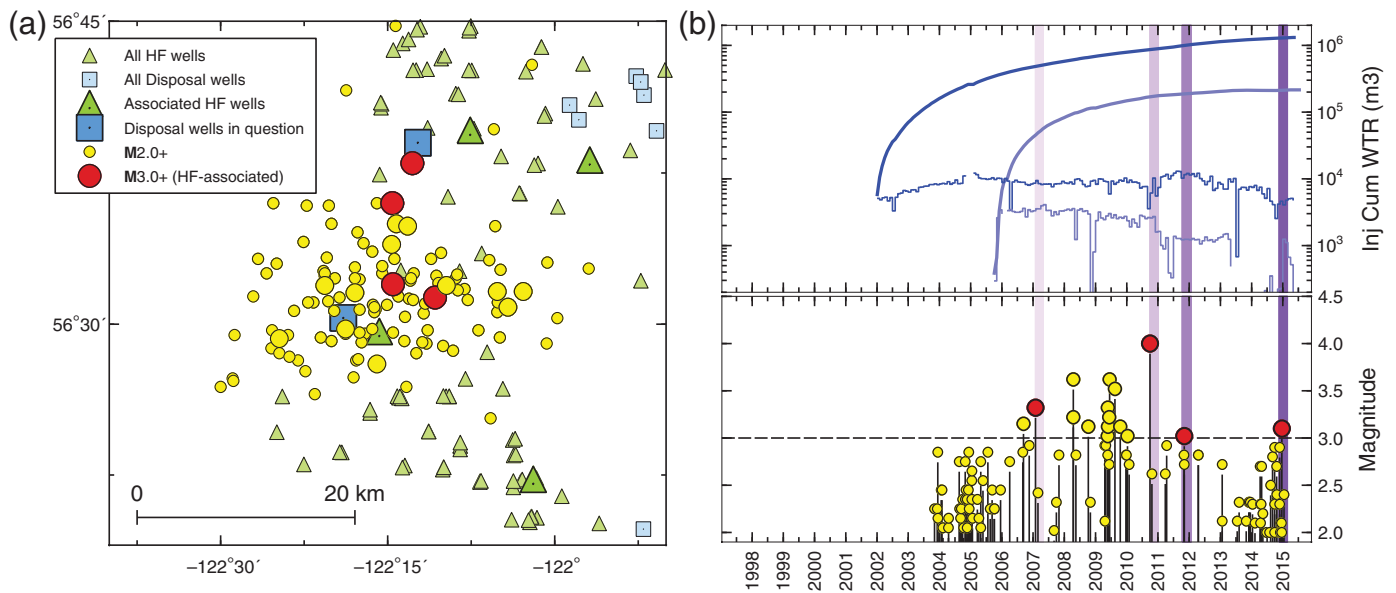


▲ **Figure 5.** (a) A group of disposal wells (squares) in a map plot with the events surrounding it. Events are color coded in time; (b, top) disposal volumes (i.e., cumulative injected water [m^3] and monthly injection [m^3]); (bottom) seismicity from 1976 to mid-2015.

we begin with an initial flagging of disposal wells for which events of $M \geq 3$ occurred any time after initiation of injection and within a 20 km radius, to account for the range of time and distance correlations noted in the literature for United States basins (Ellsworth, 2013; Frohlich *et al.*, 2014; Keranen *et al.*, 2014; Rubinstein and Babaie Mahani, 2015; Weingarten *et al.*, 2015). Obviously, with a time window of decades, and considering how widespread is the occurrence of disposal wells, most of the initially flagged events will be false positives. In fact, disposal wells are sufficiently widespread that most earthquakes in the WCSB might be expected to occur within 20 km of a disposal well. HF wells are even more widespread, but the short-time window for association (3 months for HF versus years for disposal), coupled with the low regional seismicity rates, means that meeting simple screening criteria by coincidence is much less of an issue for HF wells than for disposal wells. Thus, Monte Carlo tests of how often earthquakes occur nearby are not as diagnostic for disposal wells as they were for HF wells, and we take a different approach.

Out of 1236 disposal wells, we found that 57 have $M \geq 3$ events within 20 km. Because of the long time frame of disposal-induced seismicity, we examine all potential disposal-well correlations on an individual basis. For each of the disposal wells with $M \geq 3$ events within 20 km, we examine the seismicity in the area around the disposal wells in time and space, as illustrated in Figure 5. We examine closely spaced disposal wells (within ~ 20 km of each other) as a group. The grouping is necessary because the time window for potential correlation is very broad for disposal wells, and the uncertainties in event locations are significant; thus we are unable to distinguish which of several closely spaced disposal wells may be associated with the observed seismicity. This was not as significant an issue for closely spaced HF wells, due to the timing restrictions for association.

We consider the seismicity likely to be correlated with disposal if it initiates sometime after disposal begins in an area that previously had much lower seismicity rates. We judge the disposal wells to be uninvolved if nearby areas experience similar seismicity, or if the seismicity represents an isolated event. Four disposal wells are associated with $M \geq 3$ seismicity, on the basis of evolution of a seismicity sequence following significant disposal volumes, and for which HF wells are not involved. In addition, we identified six disposal wells where the combination of disposal and HF wells may be involved (as discussed in the section that identified 18 HF wells with nearby seismicity, where disposal wells were also located nearby. Figure 6 shows an example). Most of the larger events occurred during an HF window (and if we consider that some of the HF windows may be missing in the database, it is possible that all of the $M > 3$ events were within HF windows). This suggests the potential for important interactions within the crust's fracture network between fluids and pore pressure from wastewater disposal and the subsequent initiation of events by HF. Such preconditioning of faults by fluid injection has been detected in the central United States using matched-filtering analysis (van der Elst *et al.*, 2013). In this study, we counted the disposal well as being associated with seismicity (and not the HF wells) in Table 1 (when counting wells). However, in counting the number of associated earthquakes, we considered that both operations may play a role; we therefore counted ambiguous events that occurred in an HF window, but near a disposal well, as $\frac{1}{2}$ in both the HF-associated and disposal-associated event counts (e.g., the four events in the HF windows in Fig. 7 are counted at $\frac{1}{2}$ for disposal and $\frac{1}{2}$ for HF wells, whereas the remaining $M \geq 3$ events are counted as disposal related). It may be that in some areas that are prone to triggered seismicity, either a disposal well or a HF well, or a combination of the two, can provide such a trigger.



▲ **Figure 6.** (a) Disposal wells in a map plot with the surrounding events. $M > 3$ events that might be associated with both HF and disposal wells are shown with red circles; (b, top) disposal volumes [i.e., cumulative injected water (m^3) and monthly injection (m^3)]; (bottom) seismicity from 1998 to mid-2015. Vertical purple bars show a 3-month time window after fracturing completion for the possibly associated HF wells (shown with large green triangles at left).

In some inactive areas with poor network coverage, we recognize that the occurrence of a single-recorded $M \geq 3$ event near a disposal well might signal a significant relationship. These ambiguous events we designate as “possibly associated-disposal.” In counting the number of disposal wells with associated seismicity, we count each well (or well group) that is associated with an isolated event as $\frac{1}{2}$ (Table 1); 14 such wells are evident. We acknowledge that a significant element of subjectivity exists in the simple association between disposal wells and seismicity used here, and we have not attempted to look at every potential case in detail. The sole purpose of this exercise is to allow an initial comparison of the incidence of seismicity associated with disposal to that of seismicity associated with HF wells. More detailed follow-up studies can address the correlation between specific disposal wells and seismicity.

In total, we count 17 disposal wells (or $\sim 1\%$ of the 1236 disposal wells) as being associated with $M \geq 3$ seismicity (=4 clear cases + 6 cases in which HF wells are also nearby + 14/2 wells with ambiguous or isolated events). The average distance from a disposal well to the closest event associated with that well is 14 km (standard deviation of 11 km). This is considerably tighter than the initial 20-km screening criterion, and reasonable considering typical location uncertainties.

One event of note that we flagged as being potentially associated with disposal (counted as $\frac{1}{2}$), but which remains ambiguous, is the 2001 earthquake of M 5.4 east of Dawson Creek, British Columbia. This event occurred in proximity to a large-volume acid-gas disposal facility, and the volume of gas injected to 2001 is consistent with the magnitude (Fig. 4). However, a regional moment tensor analysis (Zhang *et al.*, 2015) has estimated the focal depth of this event to be near 15 km. Moreover, it is a relatively isolated event rather than

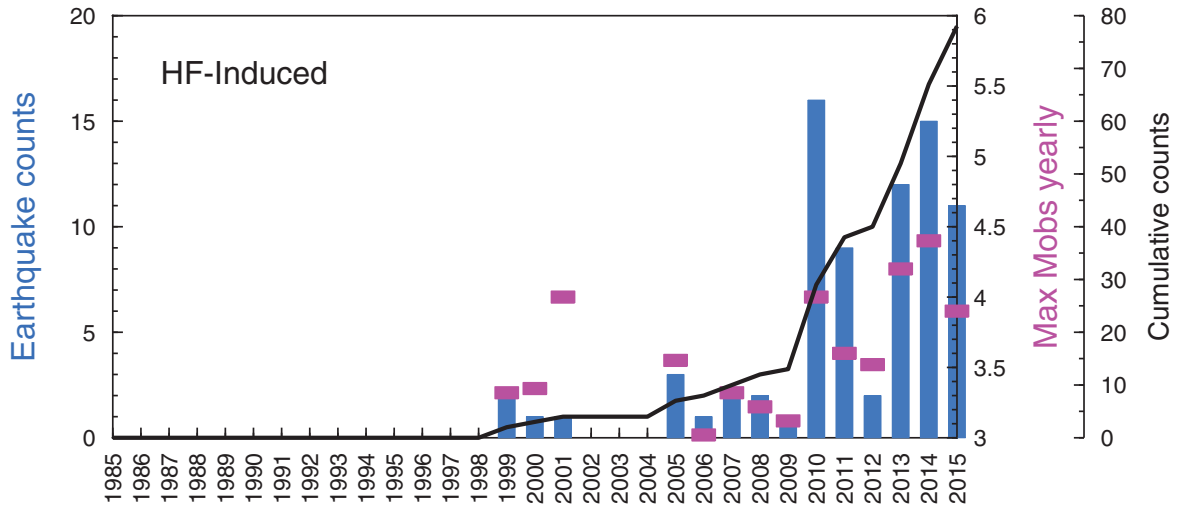
a cluster of seismicity. On the other hand, the moment tensor analysis is not well constrained. We therefore consider the cause of this event to be uncertain (classed as “possibly associated-disposal”).

Interestingly, our screening flags the seismicity in the Rocky Mountain House area of Alberta (near 52.5° N, 115° W) as being associated with disposal wells in the area. Moreover, based on timing, some very recent events in this area may have been related to hydraulic fracturing. We note previous evidence (Wetmiller, 1986; Baranova *et al.*, 1999) that events near Rocky Mountain House have been triggered by poroelastic effects due to reservoir depletion. We surmise that there may be multiple triggering mechanisms for seismicity in this area. It is also possible that, despite the well-by-well inspection process, some of the seismicity that we associated with disposal wells is actually attributable to other causes. For example, in this study we did not attempt to associate seismicity with production wells, even though production may be a contributing factor (Wetmiller, 1986; Baranova *et al.*, 1999). The simple statistical methodology that we employ would not be suitable for such a task, given the vast number of production wells and relatively low incidence of regional seismicity. Hence, more detailed study of production-related seismicity is needed.

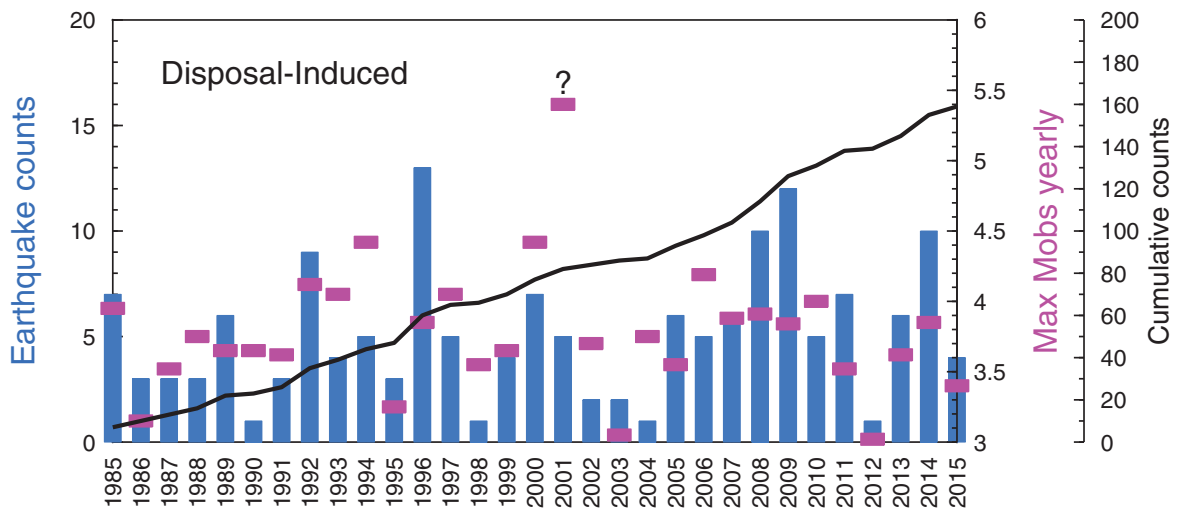
SUMMARY OF ASSOCIATION STATISTICS

Figure 1 maps the events that are associated with HF wells and disposal wells, following secondary screening. Associated statistics are summarized in Table 1. In total, we find that 39 HF wells ($\sim 0.3\%$ of 12,289 candidate HF wells) are identified as associated with seismicity at the $M \geq 3$ level, with a maximum magnitude to date of M 4.6. Similarly, we identified 17 disposal

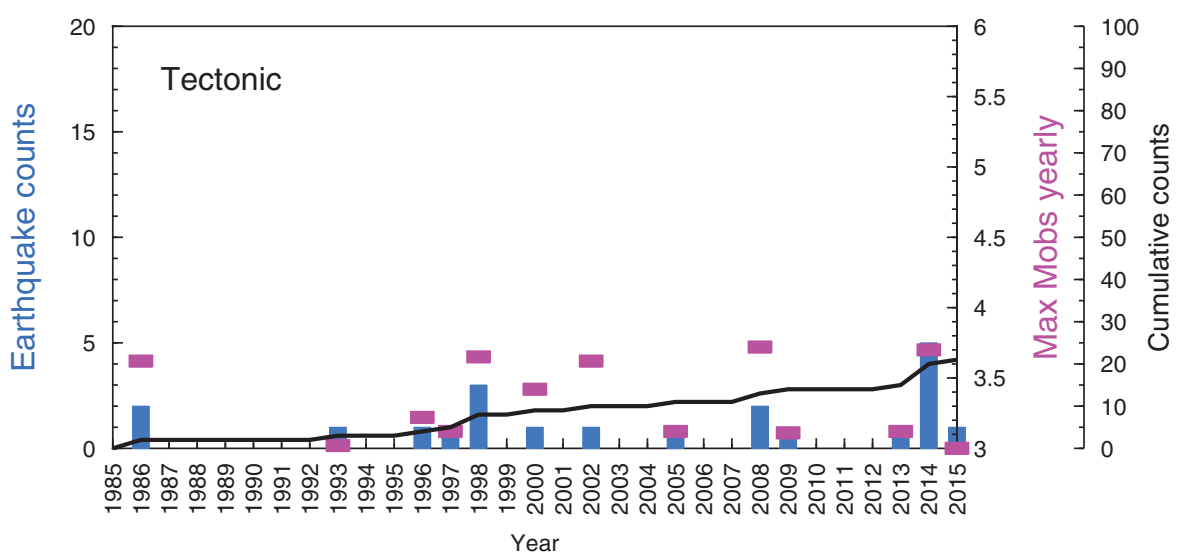
(a) Rates of $M \geq 3.0$ and maximum magnitudes observed yearly in the WCSB



(b)



(c)



▲ **Figure 7.** Annual rates of $M \geq 3$ events in the WCSB (blue bars) associated with (a) hydraulic fracturing, (b) wastewater disposal, and (c) presumed tectonic events (bottom). Black lines show cumulative count. Pink squares show the maximum observed magnitude for each category in each year. Some of the seismicity that is classified as disposal-associated may include events related to hydrocarbon production.



well locations ($\sim 1\%$ of 1236 candidates) that appear to be associated with seismicity at the $M \geq 3$ level; the largest magnitude for disposal-induced events observed to date in western Canada is $M 4.5$, but could be as high as $M 5.4$ if the enigmatic 2001 Dawson Creek event is classified as disposal-induced. Our classification of each well following evaluation of temporal plots such as those shown in the foregoing is given in the candidate-well database (see [Data and Resources](#)); we also provide the database of $M \geq 3$ events in the study area and their classifications. An interesting and important point is that while the per-well rate of association of disposal wells with seismicity is higher than that for HF wells, the number of associated events is actually greater for HF wells, because they are so much more widespread than disposal wells. This observation has important implications for hazard assessment and mitigation.

In associating seismicity with oil and gas operations (Table 1), it is not our intent to definitively classify each individual event as induced (associated) or tectonic (not associated); for many events the evidence is insufficient for conclusive identification. Rather, our aim is to assess the overall incidence of seismicity at the $M \geq 3$ level and the relative frequency of different potential causative mechanisms. We selected this threshold magnitude level because the catalog is considered to be complete above this level since 1985 (Adams and Halchuk, 2003). Moreover, $M \geq 3$ represents a level of ground shaking that is sufficiently strong to be felt at close distances (Atkinson *et al.*, 2014) and thus might be considered the minimum magnitude level of interest.

We note that the association rates determined here apply to the study region as a whole. We would expect that in reality the association rate would vary significantly within the region, according to geologic and operational variables such as the state of stress, orientation of local faults, and so on. Further research will develop a more refined model that can account for these factors and can delve into the nature and causation of the observed correlations.

Figure 7 shows the relative contributions of HF wells, disposal wells, and tectonic events to observed seismicity in the WCSB as a function of time, including an indication of the maximum sizes of events to date. A salient feature is that seismicity associated with HF wells has increased markedly since 2010, whereas the seismicity rates associated with disposal wells and tectonic events have remained nearly constant. Moreover, the maximum observed magnitudes for all three mechanisms (HF wells, disposal wells, tectonic events) appear to be similar. The relatively stationary rate of inferred tectonic events (those unassociated with oil and gas) provides independent support for our approach. In contrast, the rate that we infer for events associated with hydraulic fracturing has increased sharply in recent years, as this technology has become widespread.

DISCUSSION AND CONCLUSIONS

It is remarkable that, since 1985, most of the observed $M \geq 3$ seismicity in the WCSB appears to be associated with oil and gas activity. From 2010 to 2015, during the time period for

which both seismicity rates and the number of HF wells rose sharply, more than half of all $M \geq 3$ seismicity has occurred in close proximity to hydraulic fracturing operations in both time and space. The spatiotemporal relationship of the increased incidence of seismicity with HF wells implies that within the WCSB a greater fraction of induced seismicity (since 2010) is linked to hydraulic fracturing than to wastewater injection (Table 1), even though the per-well incidence rate is lower ($\sim 0.3\%$ versus 1%). This finding has critical implications for the distribution of hazard and the assessment of risk to the public and infrastructure. This is so even if the maximum magnitude of such events proves to be volume limited, because hazard is generally more sensitive to occurrence rate, b -value, and minimum magnitude than it is to maximum magnitude (Atkinson, Ghofrani, and Assatourians, 2015). Hazard and exposure are key elements to consider in guiding regulatory policy and field-development strategies so as to balance risks and benefits in the exploitation of oil and gas resources (Walters *et al.*, 2015). We note that our findings for the WCSB contrast markedly with other recent studies, which attribute virtually all of the increase in injection-induced seismicity in the central United States to wastewater disposal (Ellsworth, 2013; Frohlich *et al.*, 2014; Keranen *et al.*, 2014; Hornbach *et al.*, 2015; Rubinstein and Babaie Mahani, 2015; Weingarten *et al.*, 2015).

It is important to acknowledge that associated seismicity occurs for only a small proportion ($\sim 0.3\%$) of HF operations. However, considering that thousands of such wells are drilled every year in the WCSB, the implications for hazard are nevertheless significant (Atkinson, Ghofrani, and Assatourians, 2015), particularly if multiple operations are located in close proximity to critical infrastructure. The nature of the hazard from hydraulic fracturing is significantly different than that from wastewater injection. Wastewater injection involves lateral diffusion through a permeable layer over a broad area and long time frame, sometimes decades (Keranen *et al.*, 2013, 2014). In the case of HF operations, high injection rates and the relatively large spatial footprint of the stimulated region produces transient risks that may be compounded by multiple operations that are proximate in time and space.

The nature of the hazard from hydraulic fracturing has received less attention than that from wastewater disposal, but it is clearly of both regional and global importance. It is important regionally because hydraulic fracturing is widespread throughout the WCSB, an area of previously low seismicity in which seismic design measures have consequently been minimal. The likelihood of damaging earthquakes and their potential consequences needs to be carefully assessed when planning HF operations in this area. In the United States basins where the pace of development has been even greater, previous assertions that hazards from HF wells are negligible (National Research Council, 2013) warrant re-examination. In particular, it is possible that a higher-than-recognized fraction of induced earthquakes in the United States are linked to hydraulic fracturing, but their identification may be masked by more-abundant wastewater-induced events. Finally, there may be a significant induced-seismicity hazard in other countries in

the future as hydraulic fracturing well completions are increasingly used to stimulate production. Many developing countries have high exposure due to their population density, coupled with very vulnerable infrastructure (Bilham, 2009). A significant increase in the number of moderate earthquakes in developing countries would almost certainly increase the incidence of earthquake damage and fatalities.

Our results indicate that the maximum magnitude of induced events for hydraulic fracturing may not be well correlated with net injected fluid volume. Moreover, the potential occurrence of earthquakes weeks to months after a treatment program has finished implies that current mitigation strategies may require re-examination. For example, a recent event of M 4.1 induced by hydraulic fracturing south of Fox Creek, Alberta (13 June 2015) was attributed by the operator to hydraulic fracturing that was completed 8 days earlier (Tye, 2015). Thus, fluid flowback and/or traffic-light protocols, while beneficial, may not have immediate effect in preventing the occurrence of further injection-induced events (Giardini, 2009). Our understanding of the cumulative effects of multiple-hydraulic fracturing operations conducted in close proximity, as well as the magnitude distributions and temporal characteristics of the induced sequences, remains incomplete. More comprehensive characterization of the distinctive characteristics of seismicity induced by hydraulic fracturing is needed to support development of appropriate risk reduction strategies (Walters *et al.*, 2015).

DATA AND RESOURCES

The database of $\sim 500,000$ wells (all types) from 1985 to 4 June 2015, as obtained from the Alberta Energy Regulator and the B.C. Oil and Gas Commission, was searched using geoSCOUT software (geologic systems Ltd.) licensed to Western University. The earthquake database was compiled from the Composite Seismicity Catalogue for Alberta and British Columbia for the 1985 to 4 June 2015 time period, available at www.inducedseismicity.ca (last accessed November 2015). We made both the well and earthquake databases for the analyses conducted in this study available for download at www.inducedseismicity.ca/SRL (last accessed March 2016). Earthquake catalog simulations were performed using the EQHAZ1 algorithm of Assatourians and Atkinson (2013), available at www.seismotoolbox.ca (last accessed November 2015). ☒

ACKNOWLEDGMENTS

This work is supported by a collaborative development project funded by the Natural Sciences and Engineering Research Council of Canada, TransAlta, and Nanometrics. We are grateful to our colleagues and students in the Canadian Induced Seismicity Collaboration (see [Data and Resources](#)), and in particular to the work of Azadeh Fereidouni and Luqi Cui on catalog compilation. Western University thanks geoLOGIC Systems, Ltd., for the donation of geoSCOUT software licenses. We thank Art McGarr and Ben Edwards for constructive reviews of the draft manuscript.

REFERENCES

- Adams, J., and S. Halchuk (2003). Fourth generation seismic hazard maps of Canada: Values for over 650 Canadian localities intended for the 2005 National Building Code of Canada, *Geol. Surv. Canada Open-File Rept.* 4459, 150 pp.
- Assatourians, K., and G. Atkinson (2013). EqHaz: An open-source probabilistic seismic hazard code based on the Monte-Carlo simulation approach, *Seismol. Res. Lett.* **84**, 516–524.
- Atkinson, G., K. Assatourians, B. Cheadle, and W. Greig (2015). Ground motions from three recent earthquakes in western Alberta and north-eastern British Columbia and their implications for induced-seismicity hazard in eastern regions, *Seismol. Res. Lett.* **86**, 1022–1031.
- Atkinson, G., H. Ghofrani, and K. Assatourians (2015). Impact of induced seismicity on the evaluation of seismic hazard: Some preliminary considerations, *Seismol. Res. Lett.* **86**, 1009–1021.
- Atkinson, G., B. Worden, and D. Wald (2014). Intensity prediction equations for North America, *Bull. Seismol. Soc. Am.* **104**, 3084–3093.
- Baranova, V., A. Mustaqeem, and S. Bell (1999). A model for induced seismicity caused by hydrocarbon production in the Western Canada Sedimentary basin, *Can. J. Earth Sci.* **36**, 47–64.
- Bilham, R. (2009). The seismic future of cities, *Bull. Earthq. Eng.* **7**, 839–887.
- Ellsworth, W. (2013). Injection-induced earthquakes, *Science* **341**, 1225–1226.
- B.C. Oil and Gas Commission (2012). *Investigation of Observed Seismicity in the Horn River Basin*, <https://www.bcogc.ca/node/8046/download> (last accessed March 2016).
- B.C. Oil and Gas Commission (2014). *Investigation of Observed Seismicity in the Montney Trend*, <https://www.bcogc.ca/node/12291/download> (last accessed March 2016).
- B.C. Oil and Gas Commission (2015). *August Seismic Event Determination*, Industry Bulletin 2015–32, <https://www.bcogc.ca> (last accessed March 2016).
- Cornell, C. (1968). Engineering seismic risk analysis, *Bull. Seismol. Soc. Am.* **58**, 1583–1606.
- Dutta, N., and H. Ode (1979). Attenuation and dispersion of compressional waves in fluid-filled porous rocks with partial gas saturation (white model), Part I: Biot theory, *Geophysics* **44**, 1777–1788.
- Eaton, D., and A. Babaie Mahani (2015). Focal mechanisms of some inferred induced earthquakes in Alberta, Canada, *Seismol. Res. Lett.* **86**, doi: [10.1785/0220150066](https://doi.org/10.1785/0220150066).
- Eaton, D., and C. Perry (2013). Ephemeral isopycnicity of cratonic mantle keels, *Nature Geosci.* **6**, 967–970.
- Energy Information Administration (2013). *Technically Recoverable Shale Oil and Shale Gas Resources: An Assessment of 137 Shale Formations in 41 Countries Outside the United States*, <http://www.eia.gov/analysis/studies/worldshalegas> (last accessed July 2015).
- Farahbod, A., H. Kao, J. Cassidy, and D. Walker (2015). How did hydraulic-fracturing operations in the Horn River Basin change seismicity patterns in northeastern British Columbia, Canada? *TLE* **34**, 658–663.
- Frankel, A. (1995). Mapping seismic hazard in the central and eastern United States, *Seismol. Res. Lett.* **66**, no. 4, 8–21.
- Frohlich, C., W. Ellsworth, W. Brown, M. Brunt, J. Luetgert, T. MacDonald, and S. Walter (2014). The 17 May 2012 M 4.8 earthquake near Timpson, East Texas: An event possibly triggered by fluid injection, *J. Geophys. Res.* **119**, 581–593.
- Ge, J., and A. Ghassemi (2011). Permeability enhancement in shale gas reservoirs after stimulation by hydraulic fracturing, ARMA 11–514, presented at the *45th US Rock Mechanics Geomechanics Symposium*, San Francisco, California, 26–29 June 2011.
- Giardini, D. (2009). Geothermal quake risks must be faced, *Nature* **462**, 848–849.
- Guglielmi, Y., F. Cappa, J.-P. Avouac, P. Henry, and D. Ellsworth (2015). Seismicity triggered by fluid injection-induced aseismic slip, *Science* **348**, 1224–1226.

- Healy, J., W. Rubey, D. Griggs, and C. Raleigh (1968). The Denver earthquakes, *Science* **161**, 1301–1310.
- Holland, A. (2013). Earthquakes triggered by hydraulic fracturing in south-central Oklahoma, *Bull. Seismol. Soc. Am.* **103**, 1784–1792.
- Hornbach, M., H. DeShon, W. Ellsworth, B. Stump, C. Hayward, C. Frohlich, H. Oldham, J. Olson, M. Magnani, C. Brokaw, and J. Luetgert (2015). Causal factors for seismicity near Azle, Texas, *Nat. Comm.* **6**, 6728, doi: [10.1038/ncomms7728](https://doi.org/10.1038/ncomms7728).
- Horner, R., J. Barclay, and J. MacRae (1994). Earthquakes and hydrocarbon production in the Fort St. John area of northeastern British Columbia, *Can. J. Explor. Geophys.* **30**, 39–50.
- Keranen, K., H. Savage, G. Abers, and E. Cochran (2013). Potential induced earthquakes in Oklahoma, USA: Links between wastewater injection and the 2011 M_w 5.7 earthquake sequence, *Geology*, doi: [10.1130/G34045.1](https://doi.org/10.1130/G34045.1).
- Keranen, K., M. Weingarten, G. Abers, B. Bekins, and S. Ge (2014). Sharp increase in central Oklahoma seismicity since 2008 induced by massive wastewater injection, *Science* **345**, 448–451.
- Maxwell, S., J. Shemata, E. Campbell, and D. Quirk (2008). Microseismic deformation rate monitoring, presented at the 2008 SPE Annual Technical Conference and Exhibition, Denver, Colorado, 21–24 September, SPE 116596.
- McGarr, A. (2014). Maximum magnitude earthquakes induced by fluid injection, *J. Geophys. Res.* **119**, 1008–1019.
- Murray, K. (2013). State-scale perspective on water use and production associated with oil and gas operations, Oklahoma, *U.S. Environ. Sci. Technol.* **47**, 4918–4925.
- National Research Council (2013). *Induced Seismicity Potential in Energy Technologies*, National Academies Press, Washington, DC, <http://www.nap.edu/catalog/13355/induced-seismicity-potential-in-energy-technologies> (last accessed July 2015).
- Novakovic, M., and G. Atkinson (2015). Preliminary evaluation of ground motions from earthquakes in Alberta, *Seismol. Res. Lett.* **86**, doi: [10.1785/0220150059](https://doi.org/10.1785/0220150059).
- Petersen, M., C. Mueller, M. Moschetti, S. Hoover, J. Rubinstein, A. Llenos, A. Michael, W. Ellsworth, A. McGarr, A. Holland, and J. Anderson (2015). Incorporating induced seismicity in the 2014 United States National Seismic Hazard Model. Results of the 2014 workshop and sensitivity studies, *U.S. Geol. Surv. Open-File Rept. 2015-XXXX*.
- Raleigh, C., J. Healy, and J. Bredehoeft (1976). An experiment in earthquake control at Rangely, Colorado, *Science* **191**, 1230–1237.
- Rubinstein, J., and A. Bahaie Mahani (2015). Myths and facts on wastewater injection, hydraulic fracturing, enhanced oil recovery, and induced seismicity, *Seismol. Res. Lett.* **86**, doi: [10.1785/0220150067](https://doi.org/10.1785/0220150067).
- Schultz, R., S. Mei, D. Pana, V. Stern, Y. Gu, A. Kim, and D. Eaton (2015b). The Cardston Earthquake Swarm and hydraulic fracturing of the “Alberta Bakken” play, *Bull. Seismol. Soc. Am.* **105**, 2871–2884.
- Schultz, R., V. Stern, and Y. Gu (2014). An investigation of seismicity clustered near the Cordel Field, west central Alberta, and its relation to a nearby disposal well, *J. Geophys. Res.* **119**, 3410–3423.
- Schultz, R., V. Stern, Y. J. Gu, and D. Eaton (2015). Detection threshold and location resolution of the Alberta Geological Survey Earthquake Catalogue, *Seismol. Res. Lett.*, doi: [10.1785/0220140203](https://doi.org/10.1785/0220140203).
- Schultz, R., V. Stern, M. Novakovic, G. Atkinson, and Y. Gu (2015a). Hydraulic fracturing and the Crooked Lake Sequences: Insights gleaned from regional seismic networks, *Geophys. Res. Lett.* **42**, 2750–2758.
- Shapiro, S., and C. Dinske (2009). Fluid-induced seismicity: Pressure diffusion and hydraulic fracturing, *Geophys. Prospect.* **57**, 301–310.
- Shapiro, S., R. Patzig, E. Rothert, and J. Rindschwentner (2003). Triggering of seismicity by pore-pressure perturbations: Permeability-related signatures of the phenomenon, *Pure Appl. Geophys.* **160**, 1051–1066.
- Skoumal, R., M. Brudzinski, and B. Currie (2015). Earthquakes induced by hydraulic fracturing in Poland Township, Ohio, *Bull. Seismol. Soc. Am.* **105**, 189–197.
- Sumy, D., E. Cochran, K. Keranen, M. Wei, and G. Abers (2014). Observations of static Coulomb stress triggering of the November 2011 M 5.7 Oklahoma earthquake sequence, *J. Geophys. Res.* doi: [10.1002/2013JB010612](https://doi.org/10.1002/2013JB010612).
- Tyee (2015). *Another 4.4 Magnitude Industry Reported Quake in Alberta*, <http://thetyee.ca/News/2015/06/16/Another-Industry-Earthquake/> (last accessed November 2015).
- van der Elst, N., H. Savage, K. Keranen, and G. Abers (2013). Enhanced remote earthquake triggering at fluid-injection sites in the midwestern United States, *Science* **341**, 164–167.
- Walters, R., M. Zoback, J. Baker, and G. Beroza (2015). Characterizing and responding to seismic risk associated with earthquakes potentially triggered by saltwater disposal and hydraulic fracturing, *Seismol. Res. Lett.* **86**, doi: [10.1785/0220150048](https://doi.org/10.1785/0220150048).
- Walsh, F., and M. D. Zoback (2015). Oklahoma’s recent earthquakes and saltwater disposal, *Sci. Adv.* **1**, e1500195, doi: [10.1126/sciadv.1500195](https://doi.org/10.1126/sciadv.1500195).
- Weingarten, M., S. Ge, J. Godt, B. Bekins, and J. Rubinstein (2015). High-rate injection is associated with the increase in U.S. mid-continent seismicity, *Science* **348**, 1336–1344.
- Wetmiller, R. J. (1986). Earthquakes near Rocky Mountain House, Alberta, and their relationship to gas production facilities, *Can. J. Earth Sci.* **23**, 172–181.
- Zhang, H., D. Eaton, R. Harrington, and Y. Liu (2015). Discriminating induced seismicity from natural earthquakes using moment tensors and source spectra, *J. Geophys. Res.* **121**, doi: [10.1002/2015JB012603](https://doi.org/10.1002/2015JB012603).

APPENDIX

DIFFUSION OF PORE PRESSURE FOR HYDRAULIC FRACTURE WELLS AND DISPOSAL WELLS.

Pore-pressure diffusion modeling was conducted to obtain insight into the time and distance range over which a multistage HF well may influence pore pressures on proximate faults. We obtain a numerical solution to the diffusion equation:

$$\frac{\partial p}{\partial t} = \frac{\partial}{\partial x_i} \left[\mathbf{D}_{ij} \frac{\partial}{\partial x_j} p(t, \mathbf{x}) \right], \quad (\text{A1})$$

in which p denotes the pore-pressure perturbation relative to the reservoir pressure and \mathbf{D} is the diffusivity tensor. For a poroelastic medium, the diffusivity tensor is given by (Dutta and Ode, 1979):

$$\mathbf{D} = N\mathbf{K}/\eta, \quad (\text{A2})$$

in which \mathbf{K} is the permeability tensor, η is the pore-fluid dynamic viscosity, and N is a poroelastic modulus that is defined as follows (Shapiro *et al.*, 2003): $N = MP_d/H$; $M = [\phi/K_f + (\alpha - \phi)/K_g]^{-1}$; $\alpha = 1 - K_d/K_g$; $H = P_d + \alpha^2 M$; $P_d = K_d + 4/3\mu_d$; $K_{f,d,g}$ are bulk moduli of the fluid, dry frame, and grain material, respectively; μ_d is the shear modulus of the frame; and ϕ is the porosity. Values used for our simulations are listed in Table A1.

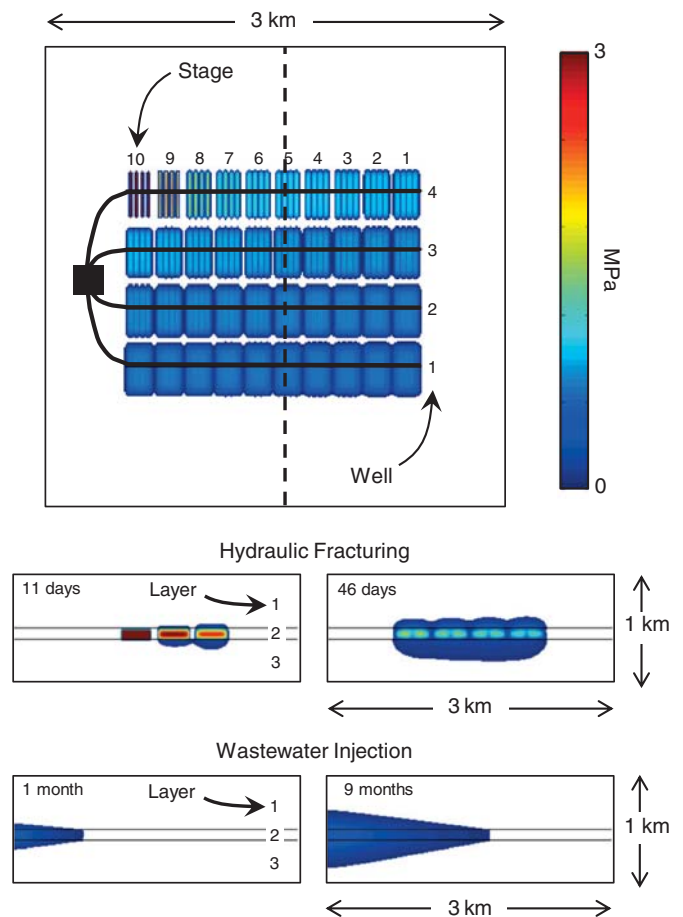
Here, we assume that \mathbf{K} is isotropic and thus can be represented as $\kappa\mathbf{I}$, in which κ is scalar permeability and \mathbf{I} is the identity matrix. We use an explicit, second-order finite-difference method to solve (1) using a 3D Cartesian coordinate system in the case of hydraulic fracturing. For simulation of wastewater disposal, we use a cylindrical coordinate system based on the same finite-difference algorithm (Eaton and Perry, 2013).

Parameter	Symbol	Unit	Value
Fluid dynamic viscosity*	η	Pa·s	1.9×10^{-4}
Dry frame modulus	K_d	Pa	4.9×10^{10}
Grain modulus	K_g	Pa	7.5×10^{10}
Fluid modulus	K_f	Pa	2.2×10^9
Frame shear modulus	μ_d	Pa	2.25×10^{10}
Porosity	ϕ	%	10

*Dynamic viscosity of salt water at 150°C.

Our representation of a multistage, multiwell hydraulic fracturing completion contains four horizontal wells that are 2000 m long, with 10 treatment stages per well and an interwell separation of 400 m, as shown in Figure A1. This configuration is representative of multiwell, multistage hydraulic fracturing programs in the Horn River basin (B.C. Oil and Gas Commission, 2012). For the hydraulic fracturing run, the unconventional reservoir is represented by a low-permeability shale that is 100 m thick and bounded, top and bottom, by more permeable formations. Each treatment stage has an injection duration of 3.3 hr, producing a stimulated rock volume (SRV) of $9.6 \times 10^5 \text{ m}^3$, represented by an 80-m high system of vertical fractures extending 150 m orthogonally in both directions from the well. Within the SRV, the pore-pressure perturbation (relative to pretreatment formation pore pressure) is maintained at 10 MPa during injection, after which the diffusivity within the SRV is increased by a factor of 10. This value was selected based on the median level of permeability enhancement due to hydraulic fracturing as determined by Ge and Ghassemi (2011). Considering 24-hr operations and a 6.7 hr interval between each stage, the simulated 40-stage HF program requires 400 hr to complete. After the injection program is complete, the relative pore pressure within each horizontal well is set to zero to simulate flowback conditions, thus producing diminishing pore pressure characterized by a back-front (Shapiro and Dinske, 2009), which diffuses slowly away from the treatment wells. For the wastewater simulation run, we used a 100-m-thick injection layer that is more permeable than the adjacent layers above and below it.

The parameters used in both runs are summarized in Table A2. For the 3D Cartesian mesh, the boundary conditions on the six outside faces of the computational grid were implemented by padding the grid with three additional rows in x , y , and z , assigning low permeability to these cells and fixing the pore-pressure perturbation at the edge of the grid to zero. For the wastewater simulation, we imposed rotational symmetry on the 2D computational grid at the lateral position of the injection ($x = 0$). At the top, bottom, and outside of the mesh we used the same approach as described above to implement boundary conditions. For all simulations, we used a grid spacing of 10 m and a time step that was adjusted to assure numerical stability of the finite difference method. In addition, prior to each run we performed multiple simulations with different grid sizes, expanding the grid dimensions until the final solu-



▲ **Figure A1.** Simulation of poroelastic diffusion. The upper frame, in map view, shows pore-pressure perturbation (scale bar in MPa) within a low-permeability formation after completion of a multistage, multiwell hydraulic fracture stimulation. The thickness of the layer is 100 m. The simulation involves 40 stages (10 per well), proceeding sequentially toward the well pad, shown by the black square, in wells 1–4, respectively. Fracture creation is approximated by a step increase in the permeability of the stimulated region upon completion of each stage. Once the entire treatment is completed, a back-front is simulated by reducing the pore-pressure perturbation to zero within each horizontal well-bore. The dashed line shows location of cross sections (middle panel), where coalescence and expansion of the pore-pressure front is depicted (left) 11 and (right) 46 days following hydraulic fracturing. The lower panel shows cross sections for a 3D simulation of wastewater disposal. The same computational method is used, but the simulation is performed using cylindrical coordinates with rotational symmetry about the injection point on the left side of the model. This scenario is representative of the expected diffusion front that accompanies massive wastewater injection into a permeable layer.

tion at the end of the modeling run had a maximum difference of less than one part per million with respect to the next smaller grid. This approach assures that the grid boundaries are sufficiently far from the region of pore-pressure perturbation to have a negligible influence on the calculated results.

Table A2
Run Parameters for Poroelectric Diffusion Models

Run	Parameter	Unit	Value
HF	κ : Layer 1	D	10^{-5}
HF	κ : Layer 2	D	10^{-6}
HF	κ : Layer 3	D	10^{-4}
HF	D : Layer 1	m^2/s	$\sim 10^{-3}$
HF	D : Layer 2	m^2/s	$\sim 10^{-4}$
HF	D : Layer 3	m^2/s	$\sim 10^{-2}$
HF	Model dimension	$x - y - z$ grid cells	$407 \times 407 \times 257$
HF	Cell size	M	10
HF	Time step	S	100 s
HF	HF fracture length	M	300
HF	HF fracture height	M	80
HF	SRV net width	M	40
HF	Fractures per stage	Unitless	4
HF	Injection excess pressure	MPa	10
WW	κ : Layer 1	D	5×10^{-6}
WW	κ : Layer 2	D	10^{-3}
WW	κ : Layer 3	D	10^{-5}
WW	D : Layer 1	m^2/s	$\sim 5 \times 10^{-4}$
WW	D : Layer 2	m^2/s	~ 0.1
WW	D : Layer 3	m^2/s	$\sim 10^{-3}$
WW	Model dimension	$r - z$ grid cells	400×107
WW	Cell size	M	10
WW	Time step	S	36 s
WW	Injection excess pressure	MPa	0.5

HF, hydraulic fracture; WW, wastewater disposal; and SRV, stimulated rock volume.

The results of our modeling are illustrated in Figure A1. In the case of hydraulic fracturing, the low initial diffusivity of the reservoir retards the expanding pulse of elevated pore pressure, but once the pressure front impinges upon a more permeable formation, the region of elevated pore pressure diffuses more rapidly away from the treatment zone. Consequently, plumes of elevated pore pressure may diffuse into formations above and below the treatment zone for a period of weeks to months. If a highly stressed fault exists outside the treatment zone, activation of the fault by increasing pore pressure will, in general, be delayed by a time interval that depends upon factors such as the diffusivity structure of the medium and proximity of HF wells to more permeable surrounding layers. In contrast, the diffusion process is simpler for continuous wastewater injection, for which the relatively high permeability of the injection layer and long duration of the disposal means that pore-pressure perturbation can diffuse readily from a point source over large distances. Overall, a single disposal well is more likely than a single HF

well to be associated with significant seismicity, and the wastewater-induced seismicity may persist over a longer period of time. However, many more HF wells exist, each of which produces a marked transient increase in pore pressure over a footprint in time and space that is dependent upon a multitude of poorly known factors. These considerations point to the importance of appropriate field-development practices that incorporate mitigation strategies for induced-seismicity hazards.

Gail M. Atkinson
Hadi Ghofrani
Burns Cheadle
Robert Shcherbakov
Kristy Tiampo
Department of Earth Sciences
Western University
London, Ontario
Canada N6A 5B7
gmatkinson@aol.com

David W. Eaton
Department of Geoscience
University of Calgary
Calgary, Alberta
Canada 2N 1N4
eaton@ucalgary.ca

Dan Walker
British Columbia Oil and Gas Commission
Victoria, British Columbia
Canada 8W 9N3

Ryan Schultz
Alberta Geological Survey
Edmonton, Alberta
Canada T6B 2X3

Jeff Gu
Mirko van der Baan
Department of Physics
University of Alberta
Edmonton, Alberta
Canada T6G 2R3

Rebecca M. Harrington
Yajing Liu
Department of Earth and Planetary Science
McGill University
Montreal, Quebec
Canada H3A 0G4

Honn Kao
Natural Resources Canada
Sidney, British Columbia
Canada V8L 6A8